Food and Bioprocess Technology (2024) 17:2678–2692
https://doi.org/10.1007/s11947-023-03284-x

RESEARCH

Antimicrobial Activity of Electrospun Nanofibers Film Incorporated with *Momordica charantia* Seed Oil for Strawberry Freshness

Caifeng Chen[1] · Yongfa Liu[1] · Abdullah[1] · Haiqiang Chen[1] · Yong Cao[1] · Yunjiao Chen[1]

Received: 13 July 2023 / Accepted: 3 December 2023 / Published online: 11 December 2023

Abstract

Momordica charantia (*M. charantia*) seeds are usually discarded; however, the oil extracted from seeds contains polyunsaturated fatty acids with potent antibacterial activity. Unfortunately, low extraction rate and instability of *M. charantia* seed oil (MCSO) limits its potential food applications. Therefore, it is crucial to explore industrial methods to increase the extraction yield and enhance stability of MCSO. Optimization of extraction process parameters for MCSO revealed a decrease in acid- and peroxide values with an α-eleostearic acid content of 41.07% ± 1.28%. Furthermore, polyvinyl alcohol/Tween-80/MCSO (PVA/T-80/MCSO) films were prepared by electrospinning, and they showed good encapsulation due to the enhancement of viscosity, electrical conductivity, fiber morphology, and intermolecular interactions. PVA/T-80/MCSO films exhibited remarkable antibacterial activities against *Escherichia coli* and *Staphylococcus aureus*, and *Caenorhabditis elegans* infected with *Pseudomonas aeruginosa* during in vitro and in vivo studies, respectively. Moreover, PVA/T-80/MCSO films successfully preserved strawberries by reducing microbial counts up to 13.8% on day 6 and controlling their moisture. This study provides new insights for the development of MCSO based natural and safe antibacterial packaging materials that could be used to enhance the quality and shelf life of food commodities.

Keywords *Momordica charantia* seed oil (MCSO) · Electrospinning · Fiber films · Natural antibacterial · Strawberries preservation

Introduction

Momordica charantia (*M. charantia*), a plant used for medicinal and culinary purposes due to its antibacterial activity (Torkamani, Syahariza, Norziah, Mahmood et al., 2018; Zubair et al., 2018), is commonly used for prevention and treatment of diseases such as inflammation, hypertension, and type 2 diabetes (Jain et al., 2018; Peter et al., 2019; Polito et al., 2016). Moreover, its seeds contain a variety of bioactive components including peptides, polyphenols, and flavonoids (Bora et al., 2023; Yoshime et al., 2016). In addition, *M. charantia* seed oil (MCSO) contains health beneficial polyunsaturated fatty acids such as conjugated trienoic acids, palmitic acids, stearic acids, and linoleic acids (Moniruzzaman et al., 2022; Vutharadhi & Nadimpalli, 2023). Notably, α-eleostearic acid is the major conjugated trienoic acid present in MCSO and exhibit potent antibacterial activity (Naik et al., 2021). Thus, MCSO is a valuable natural antibacterial resources due to high content of α-eleostearic acid (Karaman et al., 2018; Naik et al., 2021), illustrating that it is promising to be incorporated into food packaging system. However, *M. charantia* seeds are usually discarded during industrial processing, such as *M. charantia* slices and *M. charantia* juice (Gao et al., 2019; Naik et al., 2022; Yan et al., 2019), resulting in wastage of resources. Moreover, the extraction of MCSO is facing challenges such as high costs, safety concerns, unpleasant flavor, and susceptibility to oxidation, which restricts its application and development.

Traditional methods of oil extraction, such as mechanical press and soxhlet extraction have certain limitations, including low oil yields and safety issues due to solvents residues (Almeida et al., 2022; Zhao et al., 2014). To date, soxhlet

Caifeng Chen and Yongfa Liu should be considered joint first author.

✉ Yunjiao Chen
yunjiaochen@scau.edu.cn

[1] Guangdong Provincial Key Laboratory of Nutraceuticals and Functional Foods, College of Food Science, South China Agricultural University, Guangzhou 510640, Guangdong, China

extraction is the most efficient oil extraction technique due to easy processing and cost effectiveness (Gu et al., 2019). While microwave-assisted extraction, ultrasound-assisted extraction, and supercritical CO_2 method have disadvantages of high cost, complex operating conditions, and high production expenses (Danlami et al., 2014; Zhao et al., 2014). Consequently, a cost-effective and safe oil extraction technique should be developed in the long-term. Low-temperature continuous phase-change extraction (LCPE) is a novel technology developed in our laboratory for the extraction of plant-derived bioactive substances based on subcritical and supercritical extraction technology (Chen, Wang et al., 2020; Zhao et al., 2014). The principle involves compressing of extraction solvent into a liquid at a critical temperature and critical pressure. The liquid solvent then penetrates the material and extracts the target substance, before undergoing a phase-change into a gas to separate from the extracted material (Zhao et al., 2014). This extraction process can be continuously repeated (Chen, Wang et al., 2020; Zhao et al., 2014). Compared to supercritical CO_2 methods, LCPE technology not only prevents the formation of hazardous substances due to its low pressure and low temperature, but it can use a wide range of solvents, facilitating the extraction of non-polar to strongly polar substances (Chen, Yang et al., 2020; Liu et al., 2023; Zhao et al., 2014). Another advantage of LCPE technique is its continuous operation, in which the circulating solvent could produce the oil solution, ensuring efficient extraction (Chen, Yang et al., 2020; Liu et al., 2023; Zhao et al., 2014). LCPE has been utilized for extracting diverse plant bioactive substances, including finger citron essential oil (Chen, Wang et al., 2020), *Momordica* saponin (Lin et al., 2021), *Cyclocarya paliurus* polysaccharide (Lin et al., 2020), and soy sauce residue oil (Zhao et al., 2014), owing to its short extraction time, continuous extraction process, mild extraction conditions, high extraction rate, and solvent residues free extracts (Zhao et al., 2014). In this work, LCPE method was employed to optimize the conditions to extract MCSO which could possibly be used for large-scale production of MCSO.

Electrospinning is a non-mechanical fiber fabrication technique widely used to prepare nanofibers with desirable physical, mechanical, and functional attributes. In recent years, electrospinning has attracted an increasing attention of researchers to prepare loaded nanofibers due to its high loading capacity, encapsulation efficiency and desired release of loaded bioactive substances (Abdullah, Fang et al., 2022; Cheng et al., 2023; Zhang, Wang et al., 2022; Zhang, Zhang et al., 2022). The principle is that "Taylor cone" and polymer jets are formed by the interaction of the polymer solution under the high voltage electric field, these polymer jets are then stretched into flat fibers that fly towards receiver plates (Leidy & Ximena, 2019). During the flight of the jets, the solvent is evaporated, and the jets are accumulated on the receiving plate and eventually form fibers (Leidy & Ximena, 2019). The characteristics of electrospinning nanofibers, including high specific surface area, high porosity, and high encapsulation efficiency (Ansarifar et al., 2022), are helpful to tackle the issue of instability and oxidation of bioactive substances (Altan et al., 2018; Cheng et al., 2023; Zhao et al., 2014). For instance, zein nanofibers containing cinnamaldehyde essential oil were successfully prepared using electrospinning technology, which inhibited the growth of microorganisms and maintained the quality of mushrooms (Shao et al., 2019). Fish oil was encapsulated in the composite nanofibers via electrospinning technique, showing the good oxidative stability and controlled release performance (Yang et al., 2017). Above mentioned studies illustrated that electrospinning technology is an effective strategy for the encapsulation and controlled release of MCSO (Altan et al., 2018; Aytac et al., 2017). Moreover, Polyvinyl alcohol (PVA), a water-soluble polymer whose synthesis is environmentally friendly, presents excellent mechanical properties making it a suitable polymer matrix for electrospinning (Nazari et al., 2019; Wen et al., 2016; Zhang et al., 2017).

To the best of our knowledge, no published study was reported to prepare nanofiber films containing MCSO using PVA and its application as a food-active packaging. Therefore, PVA/Tween-80/MCSO (PVA/T-80/MCSO) nanofiber films were successfully prepared with MCSO encapsulated via electrospinning technique. The formed films demonstrated outstanding antibacterial activity against gram-negative and gram-positive bacteria (in vitro) and *Caenorhabditis elegans* (in vivo). Its feasibility as a food-active packaging material was explored by applying it to strawberry preservation. This study provides theoretical guidance for the development and utilization of MCSO with natural antibacterial activity.

Materials and Methods

Materials and Chemicals

M. charantia seeds were donated by Professor Dr. Kailin Hu (College of Horticulture, South China Agricultural University). *C. elegans* were purchased from the Caenorhabditis Genetics Centre. The strains of *Pseudomonas aeruginosa* (*P. aeruginosa*), *Escherichia coli* (*E. coli*), and *Staphylococcus aureus* (*S. aureus*) were stored in Guangdong Provincial Key Laboratory of Nutraceuticals and Functional Foods. PVA (MW 44.05, 87.0 ~ 89.0% hydrolysis), isooctane, potassium hydroxide, sodium bisulfate, and T-80 were purchased from Qixiang Biological Technology Co., Ltd. (Guangzhou, China); methanol, chloroform, glacial acetic acid, isopropyl

alcohol, and ethyl ether were purchased from Mingwei Biotechnology Co., Ltd. (Guangzhou, China).

Single-Factor and Orthogonal Experimental Design for Extracting of MCSO by LCPE

To examine the effects of various factors on the extraction rate of MCSO, the extraction time (30–90 min), extraction pressure (0.4–0.8 MPa), extraction temperature (30–90 °C), and analytical temperature (60–80 °C) were used as variables, respectively. The optimal technological conditions were determined by the extraction rate of MCSO.

Four factors including extraction time, extraction pressure, extraction temperature, and analytical temperature were selected as independent variables with three levels for each factor according to the design principle of orthogonal experimental (Table S1). The optimal technological conditions were determined by the extraction rate of MCSO.

Extraction Optimization and Characterization of MCSO

Preparation of MCSO

M. charantia seeds were crushed using a crusher. The powders were sieved through 40-mesh screen and loaded into the 3-L extraction kettle of the LCPE for extraction, after which the oil was removed from the kettle's outlet and weighed. The oil extraction rate was expressed as the ratio of the weight of extracted oil to the weight of raw material.

Determination of Acid Value and Peroxide Value of MCSO

Acid value and peroxide value of MCSO were determined with reference to the methods of national standards GB 5009.229-2016 and GB 5009.227-2016, respectively.

Determination of Fatty Acids in MCSO

Fatty acids were determined by gas chromatography-mass spectrometry (GC-MS) with flame ionization detector (Angelen, Santa Clara, CA, USA). Firstly, fatty acid methyl esters were prepared by dissolving 60 mg of MCSO in 4 mL of isooctane and adding 200 μL of potassium hydroxide methanol solution and 1 g of sodium bisulfate. The supernatant was taken for GC-MS analysis. The chromatographic conditions were as follows: HP-INMO-WAX capillary column, 30 m × 0.32 mm × 0.25 μm; injection volume, 1.0 μL; injector temperature, 270 °C; detector temperature, 280 °C; split ratio, 50:1. The oven was initially set at 100 °C, and the temperature was programmed to increase to 230 °C at four different rates: 0 °C/min for the first 5 min, 10 °C/min for the following 8 min and kept the temperature for 5 min, then 2 °C/min for 10 min and kept the temperature for 5 min, and 6 °C /min for the remaining 5 min. The components were identified by comparing the retention time (RT) of each component in the mass spectrometry library with that of the standards.

Preparation and Characterization of Nanofiber Films

MCSO emulsion was obtained by mixing MCSO with T-80 in a ratio of 2:1 (w/w) and adding deionized water and dissolving at 40 °C. Emulsions were prepared using a high-speed shear at 15,000 rpm/min for 10 min, followed by a high-pressure micro jet (AMH-3, ATS Engineering Limited, USA). PVA spinning solutions with 6%, 8%, 10%, and 12% (w/w) were produced by dissolving 6 g, 8 g, 10 g, and 12 g PVA in 100 g of deionized water/nanoemulsion at 50 °C for 90 min, respectively. The ratio of PVA to MCSO was set to a ratio of 4:1 (w/w).

Next, nanofilms were prepared by using electrospinning machine (Nanon-01A, MECC CO., Ltd., Japan). The prepared electrospinning solution was loaded into a 10-mL syringe fitted with an 18 G steel needle, and the injection speed was controlled by a driving pump at 0.4 mL/min. The voltage control was 18 kV and the distance between the needle and the receiver was 14 cm. The receiver consists of a collector plate covered by an earthing aluminum foil. The nanofiber film was further removed by vacuum freeze dryer (Thermo Savant) maintained for 24 h.

Determination of Films' Morphology by Using SEM

The nanofiber films surfaces were coated under vacuum using a vacuum coater (Talos L120C, FEI, USA), and the morphology of films was observed using scanning electron microscopy (SEM) (EVO MA 15, ZEISS, Germany). At least ten photographs were taken for each sample, and 120 single nanofibers (four random photographs) were analyzed using Image J software to determine the average fiber diameter.

Characterization Measurement of Films by Applying TEM

Transmission electron microscope (TEM) (Talos L120C, FEI, USA) was used to observe the microstructure of nanofiber film and the embedding of MCSO particles. The copper mesh was first placed on the aluminum foil of the collector and then spun nanofibers were placed, which were observed and photographed at different magnifications.

Characterization Measurement of Films with FTIR

Fourier Transform infrared spectroscopy (FTIR) (Vertex 70, Bruker, Germany) was used to analyze the interaction among

PVA, T-80, and MCSO. All samples were measured with attenuated total refraction (ATR) equipped with the crystal of ZnSe. The FTIR infrared spectral analysis was carried out in the wavelength range of 400–4000 cm^{-1} with a resolution of 4 cm^{-1}.

Determination of Water Contact Angle

The water contact angle of the formed nanofiber films was measured using a contact angle analyzer (SDC-100, Sheng Ding Precision Instruments Co., Ltd., Dongguan, China).

Analysis of Peroxide Value of Films

The peroxide value of films was determined by the xylenol orange method using an ultraviolet spectrophotometer (UV-1750, SHIMADZU CO., Japan). The amount of PVA/T-80/MCSO film (90 mg) was immersed in 8 mL of hexane for 1 min to remove the MCSO from the surface of the nanofiber films. The same amount of film without MCSO (90 mg) was used in the control group. The supernatant was obtained by centrifugation and the absorbance value was measured at 560 nm.

Antibacterial Properties of Nanofiber Films

Determination of In Vitro Antibacterial Activity

Antibacterial activity of nanofiber films was carried out using the disc diffusion method. Neomycin sulfate was used as a positive control and PVA nanofiber films as a negative control. Firstly, one-ring strain was inoculated in 100 mL of nutrient solution and incubated at 37 °C for 12 h at 170 rpm/min. Next, 10 mL of bacterial solution was inoculated in a new 100 mL of nutrient solution and incubated again for 12 h. The final incubation solution was obtained by diluting the bacterial liquid solution to 10^7–10^8 CFU/mL by the tenfold dilution method, which was then poured onto a plate and spread out evenly. Samples and negative controls were cut into 6.0-mm circles and irradiated with UV light for 4 h, then placed on plates and incubated at 37 °C for 24 h. Positive controls were replaced with filter paper spiked with 0.5 mg neomycin sulfate. The inhibition zone of each plate was determined. Every sample group had at least four plates and the diameters were measured three times.

Determination of In Vivo Antibacterial Activity

Lifespan tests were conducted to investigate the in vivo antibacterial activity of nanofiber films. Plates were pre-coated with *P. aeruginosa*, then samples were added, allowed to dry and sealed. Sixty infected nematodes were randomly selected and transferred to a new medium every 24 h from the L4 stage onwards to ensure contemporaneous incubation and adequate food for *C. elegans*. Meanwhile, the survival and mortality of *C. elegans* were recorded daily until all *C. elegans* died.

Application of Fiber Films in Strawberry Preservation

Strawberries with intact fruits, undamaged, non-moldy, similar size, weight, and color were selected and randomly divided into four groups, with 18 strawberries in each group. Blank group was used without any treatment. PVA/T-80 was the control group, meaning that pure electrospinning PVA/T-80 nanofilm were wrapped around the bottom of strawberries. MCSO group was used to treat the surface of strawberries with 0.4 g MCSO. PVA/T-80/MCSO group was treated with PVA/T-80/MCSO film placed on the bottom of strawberries. All samples were stored at 25 °C ± 2 °C.

Analysis of Microbial Counts

Samples of 1:10 strawberry pulp were made by adding strawberries and sterile saline (1:10) and stirring for 5 min. The strawberry pulp samples were diluted to 10^{-1}–10^{-5} dilutions using the serial tenfold dilution method. 1 mL of strawberry pulp sample was taken and mixed with an appropriate amount of plate counting agar medium (45 °C) and poured onto the plate to cool. The plates were inverted and incubated in the biochemical incubator at 37 °C for 48 h.

Analysis of Weight Loss Rate

Weight loss as an important indicator of the effectiveness of fiber films preservation (Cheng et al., 2023), which could be expressed as a ratio of the different value (initial strawberry weight—preserved N days strawberry weight) to the initial strawberry weight.

Statistical Analysis

All the experiments were repeated at least three times. The results were expressed as mean ± standard deviation (SD), and significance analysis was conducted by one-way ANOVA using SPSS16.0 software (IBM, Chicago, USA). The GraphPad prism 8.0.1 software was used to perform log-rank test and analyze the significance of the life curve. $P < 0.05$ was considered as significant difference.

Results and Discussion

Extraction Optimization and Characterization of MCSO

To efficiently and economically utilize the valuable resources present in *M. charantia* seeds, the laboratory-developed LCPE was used to extract MCSO due to its high extraction efficiency advantage (Zhao et al., 2014). The

extraction rate of MCSO was studied with single-factor experiments, specifically, variations in extraction time, extraction pressure, extraction temperature and analytical temperature. As illustrated in Fig. S1A, the extraction rate of MCSO was increased with the extension of the extraction time, and it was noteworthy that the extraction rate levelled off when the extraction time was exceeded 60 min, so the optimal extraction time should be 60 min from the consideration of the time cost. In addition, the MCSO displayed the highest extraction rate at an extraction pressure of 0.6 MPa, the extraction temperature of 45 °C, and the analytical temperature of 65 °C (Fig. S1B–D). Therefore, the L9 (3^4) orthogonal experimental design was adopted to determine the optimal extraction process parameters based on the result of the single-factor experiment. The sequence of factors affecting the extraction rate of MCSO was discovered to be as follows: extraction temperature > extraction pressure = extraction time > analytical temperature (Table 1). It may be explained by the following reasons: Firstly, extraction temperature was conducive to enhance the solubility of the extraction solvent on the lipid-soluble components of MCSO, which consequently increased the extraction rate of MCSO and had the greatest effect on the extraction rate of MCSO. Next, extraction pressure contributed to the liquefaction of the extraction solvent (Zhao et al., 2014) and allowed butane to penetrate *M. charantia* seeds effectively, enhancing the solubility and extraction of MCSO. Meanwhile, extraction time had a positive effect on extraction rate, which increased with extraction time before the extraction process reached final equilibrium (Chen, Wang et al., 2020; Zhao et al., 2014), but time cost and energy consumption were essential factors to be considered. Additionally, analytical temperature mainly affected the resolution rate and oil quality, less influence on the extraction rate (Chen, Wang et al., 2020; Zhao et al., 2014), so lower analytical temperature should be chosen for the same extraction rate. Hence, the optimal process parameters for MCSO extracted by LCPE were $A_1B_3C_2D_2$ comprised an extraction time of 50 min, an extraction pressure of 0.7 MPa, an extraction temperature of 45 °C, and an analytical temperature of 65 °C. The extraction rate conducted to validate the optimization model by LCPE was 36.8 ± 0.23 (Table 2). The result was not significant with that of soxhlet method (Table 2), which is the traditional and the most efficient method of oil extraction (Gu et al., 2019). Therefore, LCPE had no significant effect on the extraction rate of MCSO extraction.

Table 2 Physicochemical properties of MCSO

Items	LCPE	Soxhlet extraction method
Extraction rate (%)	36.8 ± 0.23^a	37.6 ± 0.23^a
Acid value (mg/g)	2.22 ± 0.03^a	3.25 ± 0.10^b
Peroxide value (g/100 g)	0.128 ± 0.001^a	0.531 ± 0.021^b

Different lowercase letters were significantly different between items in each row ($p < 0.05$)

Oil is vulnerable to oxygen, microorganisms and other factors during storage, causing rancidity and oxidation (Wu et al., 2022). Acid value and peroxide value are important indicators for evaluating the quality of oil (Wu et al., 2022). Therefore, both values were determined to further verify the advantage between LCPE at the optimal parameters and soxhlet extraction method. Compared to soxhlet extraction, LCPE dramatically reduced the acid value and

Table 1 Experimental results of extracting MCSO

NO.	Extraction time/min (A)	Extraction pressure/MPa (B)	Extraction temperature/°C (C)	Analytical temperature/°C (D)	Extraction rate /% (E)
1	50	0.5	40	60	34
2	50	0.6	45	65	36
3	50	0.7	50	70	36
4	60	0.5	45	70	33
5	60	0.6	50	60	33
6	60	0.7	40	65	32
7	70	0.5	50	65	33
8	70	0.6	40	70	32
9	70	0.7	45	60	37
I	106	100	98	99	
II	101	101	106	101	
III	102	105	102	101	
K1	35.3	33.3	32.7	33.0	
K2	33.6	33.6	35.3	33.7	
K3	34.0	35.0	34.0	33.7	
R	5	5	8	2	

peroxide value in MCSO (Table 2), indicating that LCPE improved the oxidative stability ascribed to low temperature and closed extraction conditions (Zhao et al., 2014), which protected the MCSO from air and light exposure. Therefore, LCPE at the optimal parameters was further verified the advantage in improving the oxidative stability of MCSO.

Normally, there are various fatty acids such as palmitic acid, stearic acid, linoleic acid, and conjugated trienoic acid in MCSO (Prashantha et al., 2009). In this study, GC-MS was applied to further analyze the composition of MCSO. The result found that MCSO mainly contained seven fatty acids, including α-eleostearic acid (41.07% ± 1.28%), stearic acid (32.20% ± 0.73%), linoleic acid (11.07% ± 0.36%), oleic acid (6.33% ± 0.25%), palmitic acid (5.76% ± 0.36%), arachidonic acid (1.19% ± 0.10%), and β-eleostearic acid (1.15% ± 0.10%) (Table 3 and Fig. S1). Among them, unsaturated fatty acids accounted for about 59.62%, of which main component was α-eleostearic acid, which possessed desirable functional activities such as antibacterial, antilipidemic, and anticancer (Braca et al., 2008; Chang et al., 2016). Therefore, MCSO was a valuable oil with a variety of biological activities and promising applications.

In summary, MCSO extracted by LCPE at optimal conditions exhibited high oxidative stability and abundant α-eleostearic acid content of over 40%, showing MCSO was a valuable source of natural oil (Yoshime et al., 2016). Therefore, LCPE technology with its characteristics of low-temperature continuous, economical, and efficient extraction provides the basis for the industrial production of MCSO (Zhao et al., 2014). Simultaneously, MCSO has significant value due to its abundant α-eleostearic acid, but it suffers from issues such as odor and susceptibility to oxidation, which limit its development and application.

Preparation and Optimization of MCSO Loaded Nanofibers Films

MCSO was encapsulated by electrospinning technology to enhance its stability and control release efficiency. Properties of spinning solution could influence the formation and morphology of fiber (Wen et al., 2017). On the one hand, sufficient polymer chain entanglement is the prerequisite for fiber formation, and viscosity could reflect the polymer chains entanglement (Wen et al., 2017; Zhang et al., 2018). On the other hand, proper electrical conductivity allows the spinning solution to be subjected to suitable electrical field forces at high pressures, forming jets, and being well-stretched (Wen et al., 2017; Zhang et al., 2018). Consequently, viscosity and conductivity were measured to explore the effect of different PVA concentrations on the properties of spinning solution. Both viscosity and conductivity of PVA spinning solutions were enhanced with increasing PVA concentration. However, when MCSO was incorporated into the PVA solutions, the viscosity of spinning solution was further increased, and conductivity was decreased (Table S2). A similar result was reported in other study that the electrical conductivity of electrospinning solutions was reduced by adding green tea essential oil (Yavari Maroufi et al., 2022). However, a contrary result was reported in another research that the conductivity of the electrospinning solution was increased by adding pomegranate peel extract (Bodbodak et al., 2021). It might be due to the different molecular polarity of materials, of which lipophilic materials' compounds were predominantly weak electrolytes or non-electrolytes, resulting in the poor conductivity of oils (Yuan et al., 2020).

Table 3 Fatty acid composition of MCSO

RT/min	Fatty acid	Relative amount/%
10.77	Palmitic acid	5.76 ± 0.36
19.76	Oleic acid	6.33 ± 0.25
20.27	Linoleic acid	11.07 ± 0.36
24.92	Stearic acid	32.20 ± 0.73
25.46	Arachidic acid	1.19 ± 0.10
37.78	α-eleostearic acid	41.07 ± 1.28
40.58	β-eleostearic acid	1.15 ± 0.10

The microscopic morphology and fiber diameter distribution of nanofiber films with different PVA concentrations were further analyzed by SEM to determine the optimum PVA concentration for PVA/T-80/MCSO fiber films. As illustrated in Fig. 1A and B, continuous fibers were formed at both 8% and 10% PVA concentrations. The reason could be that the appropriate viscosity facilitated the formation of "Taylor cones" and jets, as well as the stretching of jets and the formation of intact fibers (Zhang, Zhang et al., 2022). Alternatively, compared to that of 10% PVA, the nanofibers of 8% PVA concentration presented smooth surfaces. The reason might be that the fibers had smaller average diameters and distribution ranges, along with appropriate viscosity and conductivity, which was more conducive to the formation of continuous and stable jets (Wen et al., 2017). Nonetheless, neither uniform and stable jets nor continuous fibers could be formed at PVA concentrations of 6% and 12%. It might be because the solution viscosity was too low at lower PVA concentrations, and the entanglement among solutes was too small to stretch forming intact fibers (Yang et al., 2016). While the solution viscosity was so high at higher PVA concentrations that it could block the jets and result in the formation of coarse beaded fibers (Yang et al., 2016). Overall, 8% PVA concentration in the spinning solution was the best concentration to use in subsequent experiments.

The preparation process of MCSO fiber films was further investigated, and the loading of MCSO was crucial in the electrospinning method. As depicted in Fig. 2A, the fiber

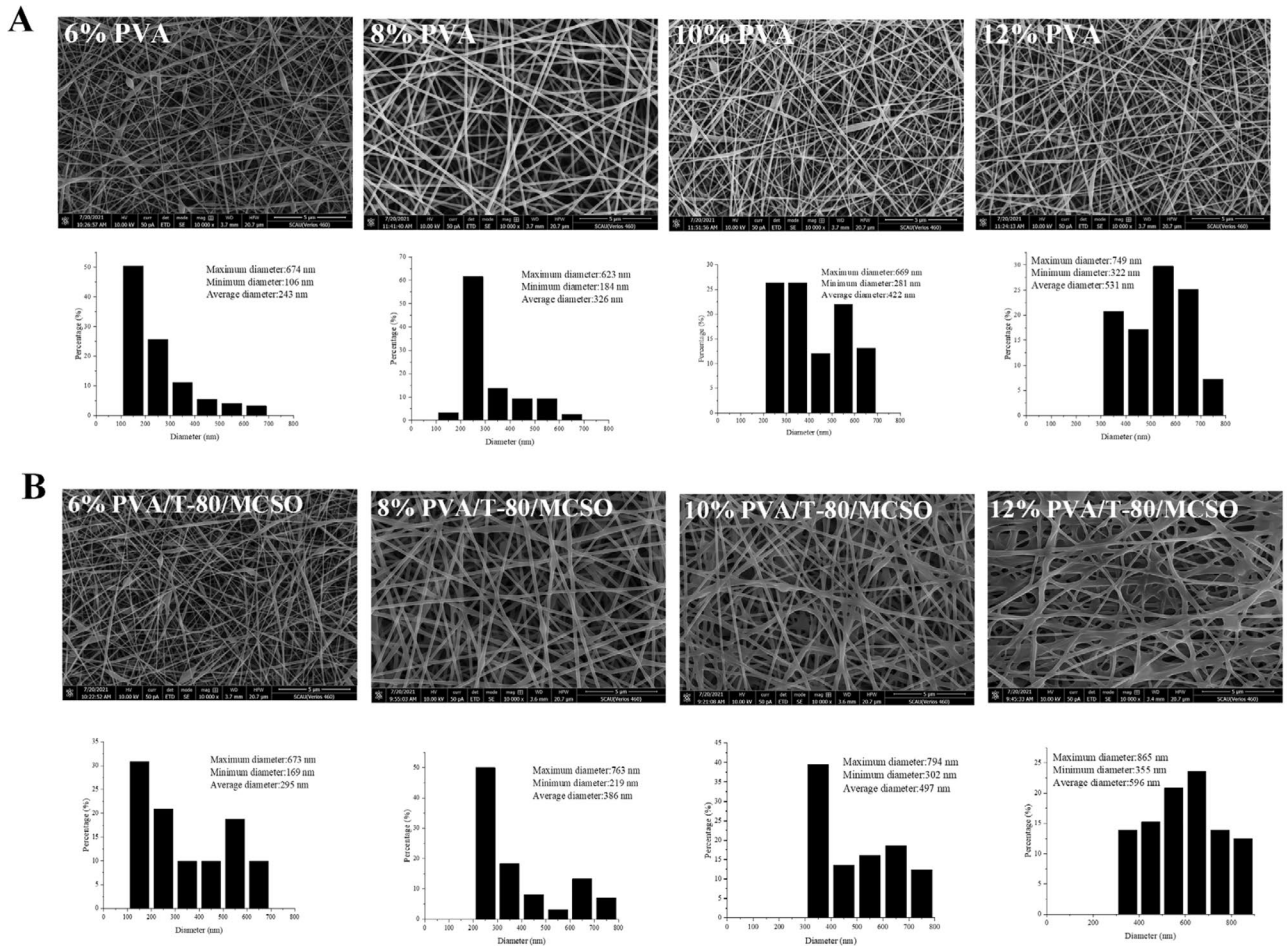

Fig. 1 SEM images and diameter distributions of **A** PVA films and **B** PVA/T-80/MCSO nanofiber films at different PVA concentrations

diameter of films was increased with the increase of MCSO concentration, and specifically was 530 nm, 590 nm, 610 nm, and 660 nm, respectively. The morphology of nanofibers was intact when the concentration of MCSO was 1% or 2%, and showed uniform distribution in fiber diameter as well as non-adhesive property because of good compatibility among PVA, T-80, and MCSO. Interestingly, it was noted that compared to 1% MCSO, a smoother and more compact fiber films of PVA/T-80/MCSO were observed at a concentration of 2% MCSO. However, when the MCSO concentration increased to 3% or 4%, the fiber diameter of the PVA/T-80/MCSO fiber films was not uniformly distributed and there was adherence among some of the fibers. It could be because spinning solution's viscosity was increased under high MCSO concentrations, which hindered the jet stretching and resulted in unsatisfactory encapsulation. Above results revealed that the PVA/T-80 film incorporated with 2% MCSO could have a good performance in fiber morphology and fiber diameter. Additionally, contact angle is an important indicator of hydrophilicity (Cheng et al., 2023). The films with a contact angle above 90° is hydrophobic, while an angle below 30° signifies that the surface is thoroughly wettable (hydrophilic), and a contact angle ranging between 30 and 90° represents that the surface is partly wettable (Yun et al., 2023). Water contact angle was assayed to investigate the effect of different MCSO concentrations on the wetting properties of the films. The contact angles of five films were increased from 69.14 ± 1.2 to $83.43 \pm 1.1°$ with increasing MCSO concentration, which reflected that these films were partially wettable (Fig. 2B). This result was similar to the results of Cheng et al. (2023). The following reasons might be given: Firstly, PVA was a typical hydrophilic material with numerous –OH groups in its structure (Cheng et al., 2023), whereas MCSO was a hydrophobic material which could fill the gaps among the fiber films. Moreover, the film's hydrophilicity could be affected by its surface morphology (Cai et al., 2021). Previous studies have shown that the surface properties of the fibers became coarser with increasing MCSO concentration (Fig. 2A), which led to an increase water contact angle. Notably, the contact angle of 1% and 2% MCSO was $72.36 \pm 0.8°$ and $76.73 \pm 0.9°$, respectively, exhibiting increased hydrophobicity compared

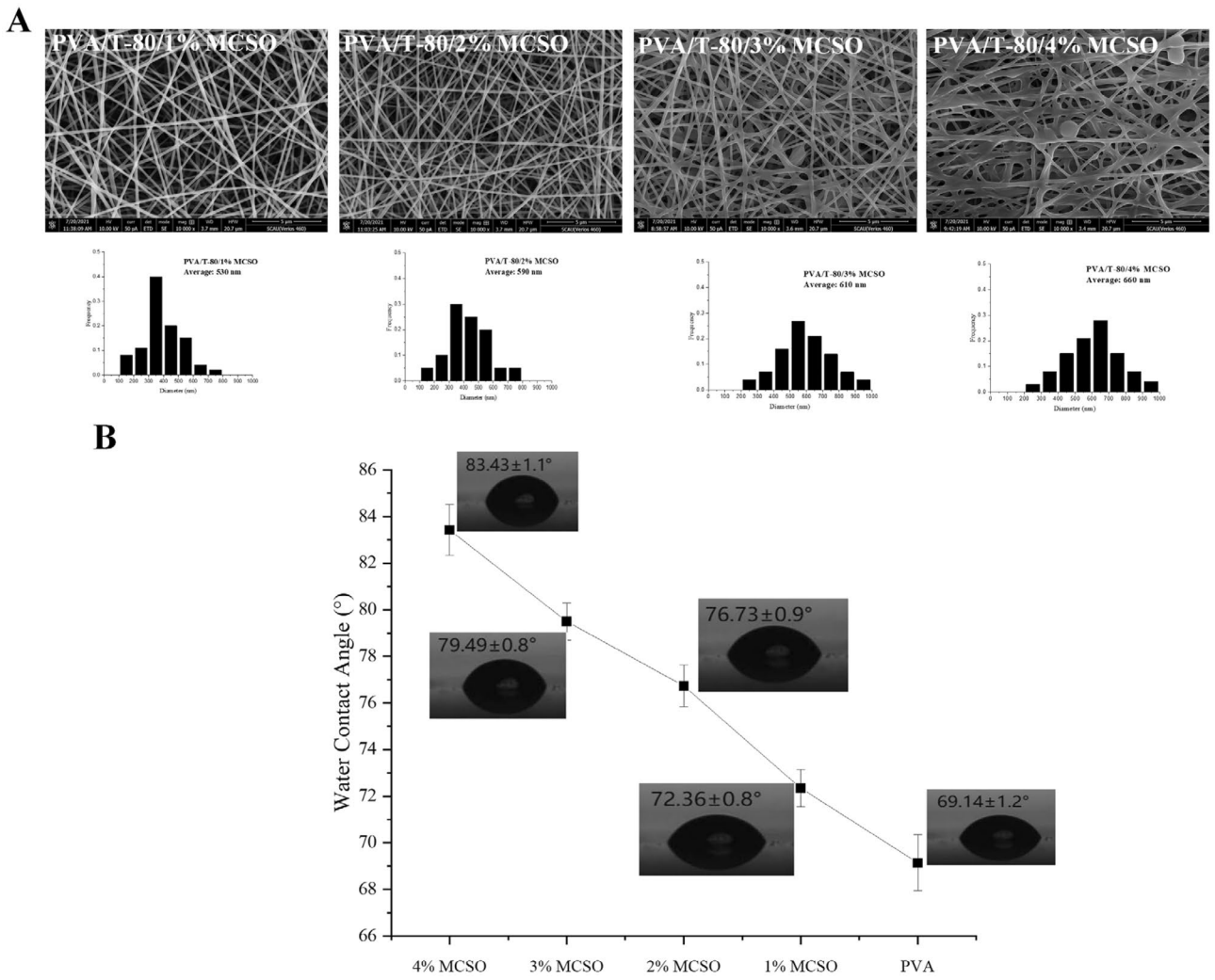

Fig. 2 **A** SEM images and diameter distribution and **B** water contact angle of PVA/T-80/MCSO nanofiber films at different MCSO concentrations

to control. Therefore, considering the fiber diameter distribution, fiber morphology, and water contact angle, PVA/T-80 films incorporated with 2% MCSO was the best choice for subsequent studies.

Collectively, based on the performance of the physical properties, SEM microstructure, diameter distribution and hydrophilicity of fiber films, the concentration of 8% PVA and 2% MCSO was chosen as the optimized formulation for the electro-spinning of PVA/T-80/MCSO fiber films.

Characterization of MCSO Loaded Nanofibers Films

FTIR was used to reflect the molecular structural features and interactions among chemical groups in MCSO-loaded PVA/T-80 films during electrospinning (Liu et al., 2021; Wen et al., 2016). As shown in Fig. 3A, PVA had characteristic peaks at 3340 cm^{-1} (O–H stretching), 2945 cm^{-1} (C–H stretching), and 1091 cm^{-1} (C–O stretching). T-80 exhibited characteristic peaks at 2931 cm^{-1} (C–H stretching) and 1029 cm^{-1} (C–O stretching). Compared to the spectra of both T-80 and PVA/T-80 films, PVA/T-80/MCSO fiber films displayed a complete disappearance of the O–H stretching peak at 671 cm^{-1}. It was possibly because more hydrogen bonds were formed among PVA, T-80, and MCSO, resulting in increasing bond lengths. It demonstrated that MCSO was encapsulated completely in the cavity of PVA/T-80. Furthermore, PVA/T-80/MCSO films had the C–O–H stretch at 1093 cm^{-1}, illustrating that interaction existed among PVA, T-80, and MCSO. Those results demonstrated that adding MCSO improved the stability of the fiber films (Wen et al., 2016).

The micro-core shell structure of PVA/T-80/MCSO fiber films was observed through TEM to further explore the encapsulation in the nanofiber films by adding MCSO.

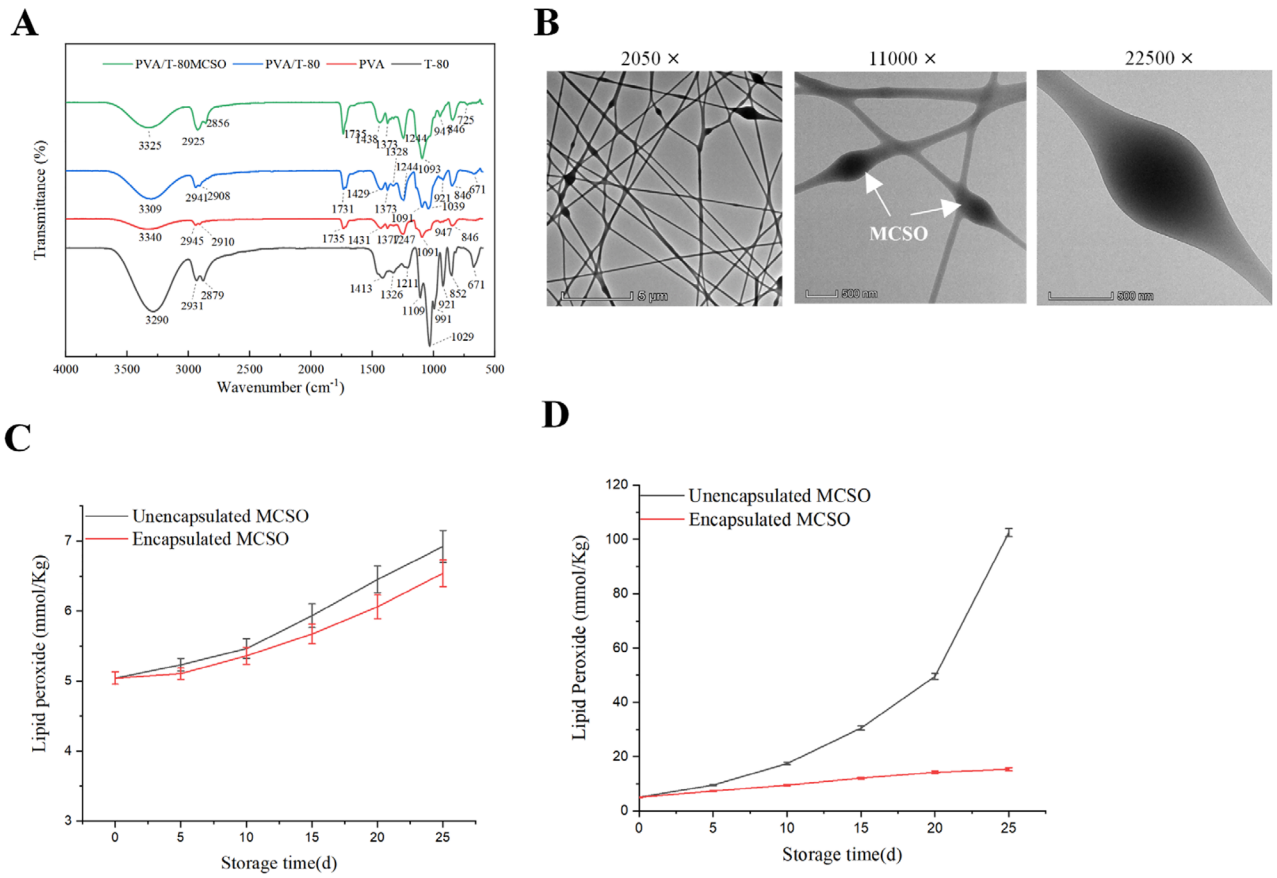

Fig. 3 Characterization of MCSO-loaded nanofibers films. **A** FTIR spectrum of fibrous membranes. **B** TEM diagram of PVA/T-80/MCSO film; the left was observed under low magnification (5 μm) and the right under high magnification (500 nm). Peroxide value of fibrous membranes under **C** anaerobic and **D** aerobic conditions

Many black nodes were observed within the interlaced fibers at low magnification (× 2050, left, Fig. 3B), which were clearly defined to normal fibers. Meanwhile, the different sizes of fibers could be observed at high magnification. First of all, a clear color difference between the black nodes and their smooth parts of the fibers was observed in the small fibers, with the middle part being darker than edges (× 11,000, middle, Fig. 3B). This might be because the outer part of nanofiber film absorbs less electrons and appears brighter, while the inner layer absorbs more electrons and appears darker (Mahmood et al., 2023). This result was similar to the results of Torkamani, Syahariza, Norziah, Wan et al. (2018). Moreover, the same results were found in the large fibers (× 22,500, right, Fig. 3B). These results revealed that MCSO was successfully encapsulated inside the fiber film by electrospinning, which also further verified that the compatibility of fiber films improved with the addition of MCSO.

Xylene phenol orange method was adopted to monitor the effect of encapsulated and unencapsulated MCSO on peroxide value under the different storage conditions to further explore the oxidative stability of nanofiber films and the embedding efficiency after adding MCSO. Peroxide value of both encapsulated and unencapsulated MCSO was increased slowly with storage time at room temperature anaerobic conditions, with no significant difference (Fig. 3C). However, compared to anaerobic conditions, the unencapsulated MCSO had higher peroxide value under aerobic conditions which increased at faster rate (Fig. 3D), suggesting that oxygen facilitated the oil's oxidative rancidity. It was worth mentioning that the encapsulated MCSO reduced the growth rate of the peroxide value.

Overall, oxidative rancidity of MCSO was affected by oxygen, but MCSO encapsulation slow down the process of oxidative deterioration. This demonstrated that MCSO was effectively encapsulated in electrospinning nanofibers and isolated from the external environment, thereby improving the oxidative stability of MCSO. Therefore, PVA/T-80/MCSO fiber films were promising delivery cargos for various industrial applications of MCSO.

Antibacterial Activity of PVA/T-80/MCSO Fiber Films

The inhibition zone diameters of PVA/T-80/MCSO fiber films were measured to evaluate the in vitro antibacterial activity against *E. coli* (gram-negative bacteria) and *S. aureus* (gram-positive bacteria). PVA/T-80 films did not show inhibition zones against *E. coli* and *S. aureus*. While both MCSO and PVA/T-80/MCSO films significantly inhibited the growth of bacteria leading to inhibition zones (Fig. 4A), illustrating that they had antibacterial ability against *E. coli* and *S. aureus*. Briefly, PVA/T-80/MCSO showed inhibition zone with diameters of 22.3 ± 0.4 mm and 20.7 ± 0.3 mm against *E. coli* and *S. aureus*, respectively (Table S3). This indicated that the PVA/T-80/MCSO fiber films had good inhibition effect, which could penetrate the cell wall of the bacteria.

P. aeruginosa is a widespread gram-negative bacterium and a common model pathogen in *C. elegans* resistance assays (Vairo et al., 2023). Hence, lifespan was determined in the model of *P. aeruginosa* infection with *C. elegans* to explore the in vivo antibacterial activity of PVA/T-80/MCSO fiber films. Compared to blank group, both MCSO and PVA/T-80/MCSO fiber films significantly shifted the lifespan curve of *C. elegans* towards the right (Fig. 4B), demonstrating that MCSO effectively reduced the virulence of *P. aeruginosa* against *C. elegans* and improved survival during infection. It was notable that PVA/T-80/MCSO fiber films showed a more prominent performance in prolonging the lifespan. The possible reasons were as follows: Firstly, the addition of MCSO enhanced the nanostructure of the fiber films, and achieved an effective release of its antibacterial activity by enhancing the interaction with the surrounding medium (Antunes et al., 2017). Secondly, more hydrogen bonds were generated with PVA and T-80 when MCSO was encapsulated inside the nanofiber films, and further increased the bond length, as well as facilitated the slow release and action of the antibacterial component present in MCSO. The data was

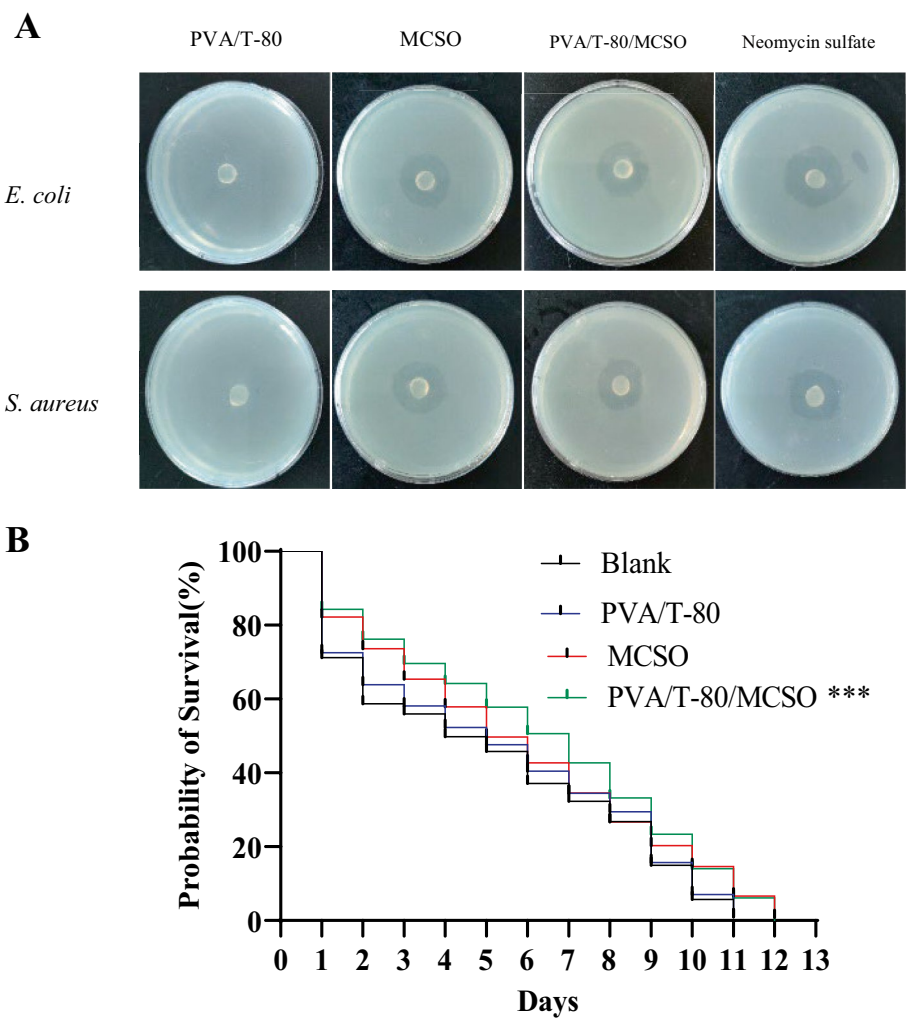

Fig. 4 Antibacterial activity of MCSO-loaded nanofibers films. **A** Inhibition zones of fiber films. **B** Effect of fiber films on lifespan of *C. elegans* infected by *P. aeruginosa*

consistent with the results of FTIR, TEM, and in vivo antibacterial activity, demonstrating that the PVA/T-80/MCSO fiber films exhibited remarkable performance during in vivo study.

Collectively, PVA/T-80/MCSO fiber films displayed good in vitro antibacterial activity against selected strains, as well as in vivo antibacterial activity by prolonging the lifespan of *P. aeruginosa* infection in *C. elegans* models. This study concluded that MCSO had promising potential as a natural antibacterial for industrial applications.

Application of PVA/T-80/MCSO Fiber Films in Strawberry Preservation

The effect of PVA/T-80/MCSO fiber films on the shelf life of strawberry was observed to further validate the long-term antibacterial effect of electrospinning fiber films. First, the surface morphology of strawberries was observed to directly analyze the antibacterial effect of the PVA/T-80/MCSO fiber films. As depicted in Fig. 5A, strawberry rot occurred in blank group on day 3, while only a few strawberries in PVA/T-80/MCSO treatment group showed smaller areas of decay on day 6. It illustrated that the PVA/T-80/MCSO fiber films effectively prevented fruit spoilage. The reason might be because the prolonging shelf life of strawberries could be induced by the antibacterial effect of the α-eleostearic acid released by MCSO (Zhang, Liu et al., 2022).

Fruits are prone to microbial spoilage during storage, and antibacterial packaging in the food field is usually used to preserve freshness by inhibiting the microbial growth (Abdullah, Cai et al., 2022; Topuz & Uyar, 2020; Zhang, Liu et al., 2022). For instance, previous studies indicated that using plant extracts with antibacterial properties in packaging materials could alleviate the microbial growth (Saadat et al., 2021; Tavassoli-Kafrani et al., 2018). Therefore, it was necessary to monitor the microbial levels of strawberries during storage to further explore the antibacterial effect of PVA/T-80/MCSO fiber films. As illustrated in Fig. 5B,

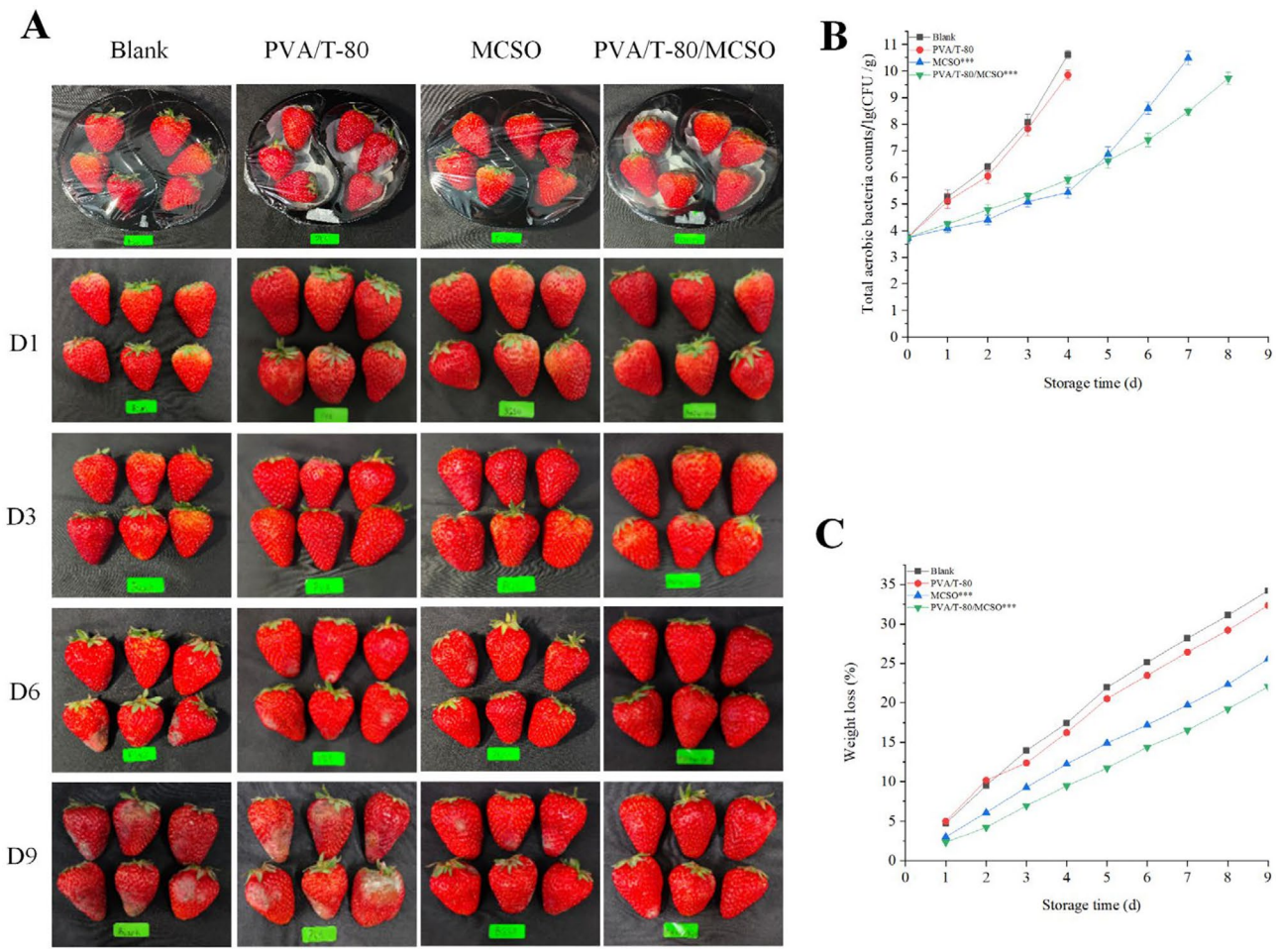

Fig. 5 **A** Strawberries with different treatment stored at 25 °C. Changes in **B** total aerobic bacteria counts (The counts of total aerobic bacteria in Blank and PVA/T-80 groups were not examined after day 5 due to microbiological exceedances after day 5.) and **C** weight loss rate with increasing preservation time of strawberries

the counts of total aerobic bacteria increased continuously. Of which, the counts of total aerobic bacteria were lower in both MCSO and PVA/T-80/MCSO film groups than in the blank and PVA/T-80 film groups. It indicated that MCSO and PVA/T-80/MCSO films significantly inhibited the microbial growth on the surface of strawberries. Notably, the counts of total aerobic bacteria in the PVA/T-80/MCSO fiber films group were significantly reduced by 13.8% compared to those in the unencapsulated MCSO group on day 6, with a stronger antibacterial effect. It was probably because the stability of fiber film was improved by the intermolecular interactions among PVA, T-80, and MCSO, as well as α-eleostearic acid was released from MCSO and inhibited the microbial growth.

Weight loss is an important parameter to evaluate the freshness of fruit preservation (Cheng et al., 2023). Weight loss of strawberries during storage is mainly due to transpiration of water and its own respiration which accelerates the consumption of organic matter (Cheng et al., 2023; Wen et al., 2016). Wounds and flower stem scars in fresh strawberries are also important contributors to water loss (Cheng et al., 2023). Thus, weight loss was determined to investigate whether PVA/T-80/MCSO fiber films extended shelf life of strawberries by controlling water loss. Weight loss rate of strawberries was increased continuously with time, especially in the blank and PVA/T-80 film groups, while PVA/T-80/MCSO fiber film group significantly decreased the weight loss rate (Fig. 5C), implying that MCSO played a major part in the effect of freshness preservation. Possible reasons were as follows: Firstly, α-eleostearic acid rich in MCSO was released during storage to effectively inhibit the growth of microorganisms on the surface of strawberries and maintained the strength of skin and prevented water loss (Cheng et al., 2023). Moreover, water transpiration from respiratory metabolism was resisted by the lipophilic nature of MCSO, resulting in slower respiration of fruits (Wen et al., 2016) and reduced weight loss for effective freshness preservation.

In summary, MCSO and PVA/T-80/MCSO fiber films prevented the spoilage of strawberries during storage; however, PVA/T-80/MCSO fiber films demonstrated superior preservation effects in slowing down surface spoilage and microbial counts of strawberries. In conclusion, MCSO played an important role as an antibacterial preservation of strawberries, while electrospinning technology effectively improved the oxidative stability and antibacterial activity of the PVA/T-80/MCSO fiber films.

Conclusion

MCSO is rich in polyunsaturated fatty acids and exhibits potent antibacterial activity. In order to efficiently utilize the valuable resources of *M. charantia* seeds and achieve the large-scale production of MCSO, MCSO was extracted by LCPE and its extract process parameters were optimized in this study. MCSO showed a low acid value and peroxide value content and had a content of α-eleostearic acid of up to 41.07% ± 1.28%. PVA/T-80/MCSO fiber films were obtained through encapsulation of MCSO using electrospinning technology. It was found that PVA/T-80/MCSO films' oxidative stability was improved, including the improvement in fiber morphology and hydrophilicity of PVA/T-80/MCSO, as well as the compatibility of the fiber films. Besides, PVA/T-80/MCSO films showed an outstanding antibacterial effect against *E. coli* and *S. aureus* (in vitro), as well as against *P. aeruginosa*-infected *C. elegans* (in vivo). These results demonstrated that PVA/T-80/MCSO fiber films were the ideal active packaging material. Importantly, PVA/T-80/MCSO fiber films maintained the freshness of strawberries, inhibited the total aerobic bacteria growth and extended the shelf life of strawberries. Our study provides a new insight for utilizing MCSO from *M. charantia* seeds at large-scale production and exploiting MCSO's antibacterial properties, which is conducive to the development of MCSO.

Supplementary Information The online version contains supplementary material available at https://doi.org/10.1007/s11947-023-03284-x.

Author Contributions CC: conceptualization, data curation, formal analysis, methodology, software, writing—original draft; YL: conceptualization, data curation, formal analysis, methodology, software, writing—original draft; A: writing—review and editing; HC: writing—review and editing; YC: writing—review and editing, investigation, validation, supervision; YC: writing—review and editing, validation, supervision, funding acquisition, project administration, resources. All authors reviewed the manuscripts.

Funding This research was supported by the General Project of the Natural Science Foundation of Guangdong Province, China (2022A1515010907; 2023A1515011266), and the National Natural Science Foundation of China (31700501).

Data Availability Data will be made available on request.

Declarations

Competing Interests The authors declare no competing interests.

References

Abdullah, Cai, J., Hafeez, M. A., Wang, Q., Farooq, S., Huang, Q., ... & Xiao, J. (2022). Biopolymer-based functional films for packaging applications: A review. *Frontiers in Nutrition*. https://doi.org/10.3389/fnut.2022.1000116

Abdullah, Fang, J., Liu, X., Javed, H. U., Cai, J., Zhou, Q., ... & Xiao, J. (2022). Recent advances in self-assembly behaviors of prolamins and their applications as functional delivery vehicles. *Critical Reviews in Food Science and Nutrition*. https://doi.org/10.1080/10408398.2022.2113031

Almeida, F. S., Dias, F. F. G., Sato, A. C. K., & De Moura Bell, J. M. L. N. (2022). Scaling up the two-stage countercurrent extraction

of oil and protein from green coffee beans: Impact of proteolysis on extractability, protein functionality, and oil recovery. *Food and Bioprocess Technology, 15*(8), 1794–1809. https://doi.org/10.1007/s11947-022-02831-2

Altan, A., Aytac, Z., & Uyar, T. (2018). Carvacrol loaded electrospun fibrous films from zein and poly(lactic acid) for active food packaging. *Food Hydrocolloids, 81*, 48–59. https://doi.org/10.1016/j.foodhyd.2018.02.028

Ansarifar, E., Hedayati, S., Zeinali, T., Fathabad, A. E., Zarban, A., Marszałek, K., & Mousavi Khaneghah, A. (2022). Encapsulation of jujube extract in electrospun nanofiber: Release profile, functional effectiveness, and application for active packaging. *Food and Bioprocess Technology, 15*(9), 2009–2019. https://doi.org/10.1007/s11947-022-02860-x

Antunes, M. D., Dannenberg, G. D. S., Fiorentini, Â. M., Pinto, V. Z., Lim, L. T., Zavareze, E. D. R., & Dias, A. R. G. (2017). Antimicrobial electrospun ultrafine fibers from zein containing eucalyptus essential oil/cyclodextrin inclusion complex. *International Journal of Biological Macromolecules, 104*, 874–882. https://doi.org/10.1016/j.ijbiomac.2017.06.095

Aytac, Z., Ipek, S., Durgun, E., Tekinay, T., & Uyar, T. (2017). Antibacterial electrospun zein nanofibrous web encapsulating thymol/cyclodextrin-inclusion complex for food packaging. *Food Chemistry, 233*, 117–124. https://doi.org/10.1016/j.foodchem.2017.04.095

Bodbodak, S., Shahabi, N., Mohammadi, M., Ghorbani, M., & Pezeshki, A. (2021). Development of a novel antimicrobial electrospun nanofiber based on polylactic acid/hydroxypropyl methylcellulose containing pomegranate peel extract for active food packaging. *Food and Bioprocess Technology, 14*(12), 2260–2272. https://doi.org/10.1007/s11947-021-02722-y

Bora, A. F. M., Kouame, K.J.E.-P., Li, X., Liu, L., & Pan, Y. (2023). New insights into the bioactive polysaccharides, proteins, and triterpenoids isolated from bitter melon (Momordica charantia) and their relevance for nutraceutical and food application: A review. *International Journal of Biological Macromolecules, 231*, 123173. https://doi.org/10.1016/j.ijbiomac.2023.123173

Braca, A., Siciliano, T., D'Arrigo, M., & Gennano, M. P. (2008). Chemical composition and antimicrobial activity of Momordica charantia seed essential oil. *Fitoterapia, 79*(2), 123–125. https://doi.org/10.1016/j.fitote.2007.11.002

Cai, J., Zhang, D., Zhou, R., Zhu, R. Y., Fei, P., Zhu, Z. Z., ... & Ding, W. P. (2021). Hydrophobic interface starch nanofibrous film for food packaging: From bioinspired design to self-cleaning action. *Journal of Agricultural and Food Chemistry, 69*(17), 5067–5075. https://doi.org/10.1021/acs.jafc.1c00230

Chang, Y. Y., Su, H. M., Chen, S.-H., Hsieh, W.-T., Chyuan, J.-H., & Chao, P.-M. (2016). Roles of peroxisome proliferator-activated receptor α in bitter melon seed oil-corrected lipid disorders and conversion of α-eleostearic acid into rumenic acid in C57BL/6J mice. *Nutrients*. https://doi.org/10.3390/nu8120805

Chen, H., Yang, H., Zhou, A., Xiao, S., Song, M., Chen, H., & Cao, Y. (2020). A novel continuous phase-transition extraction effectively improves the yield and quality of finger citron essential oil extract. *Journal of the American Oil Chemists' Society*. https://doi.org/10.1002/aocs.12433

Chen, H. Q., Wang, J., Liu, X. J., Zhou, A. M., Xiao, J., Huang, K. X., ... & Cao, Y. (2020). Optimization in continuous phase-transition extraction of crude flavonoids from finger citron fruit and evaluation on their antiaging activities. *Food Science & Nutrition, 8*(3), 1636–1648. https://doi.org/10.1002/fsn3.1450

Cheng, C. X., Min, T. T., Luo, Y. W., Zhang, Y. S., & Yue, J. (2023). Electrospun polyvinyl alcohol/chitosan nanofibers incorporated with 1,8-cineole/cyclodextrin inclusion complexes: Characterization, release kinetics and application in strawberry preservation. *Food Chemistry, 418*, 135652. https://doi.org/10.1016/j.foodchem.2023.135652

Danlami, J. M., Arsad, A., Zaini, M. A. A., & Sulaiman, H. (2014). A comparative study of various oil extraction techniques from plants. *Reviews in Chemical Engineering, 30*(6), 605–626. https://doi.org/10.1515/revce-2013-0038

Gao, H., Wen, J.-J., Hu, J.-L., Nie, Q.-X., Chen, H.-H., Nie, S.-P., ... & Xie, M.-Y. (2019). Momordica charantia juice with Lactobacillus plantarum fermentation: Chemical composition, antioxidant properties and aroma profile. *Food Bioscience, 29*, 62–72. https://doi.org/10.1016/j.fbio.2019.03.007

Gu, L.-B., Zhang, G.-J., Du, L., Du, J., Qi, K., Zhu, X.-L., ... & Jiang, Z.-H. (2019). Comparative study on the extraction of Xanthoceras sorbifolia Bunge (yellow horn) seed oil using subcritical n-butane, supercritical CO2, and the Soxhlet method. *LWT - Food Science and Technology, 111*, 548–554. https://doi.org/10.1016/j.lwt.2019.05.078

Jain, A., Sengupta, S., & De, S. (2018). Fundamental understanding of fouling mechanisms during microfiltration of bitter gourd (Momordica charantia) extract and their dependence on operating conditions. *Food and Bioprocess Technology, 11*(5), 1012–1026. https://doi.org/10.1007/s11947-018-2074-9

Karaman, K., Dalda-Şekerci, A., Yetişir, H., Gülşen, O., & Coşkun, Ö. F. (2018). Molecular, morphological and biochemical characterization of some Turkish bitter melon (*Momordica charantia* L.) genotypes. *Industrial Crops and Products, 123*, 93–99. https://doi.org/10.1016/j.indcrop.2018.06.036

Leidy, R., & Ximena, Q. C. M. (2019). Use of electrospinning technique to produce nanofibres for food industries: A perspective from regulations to characterisations. *Trends in Food Science & Technology, 85*, 92–106. https://doi.org/10.1016/j.tifs.2019.01.006

Lin, C. X., Lin, Y. Z., Xiao, J., Lan, Y. Q., Cao, Y., & Chen, Y. J. (2021). Effect of Momordica saponin- and Cyclocarya paliurus polysaccharide-enriched beverages on oxidative stress and fat accumulation in Caenorhabditis elegans. *Journal of the Science of Food and Agriculture, 101*(8), 3366–3375. https://doi.org/10.1002/jsfa.10966

Lin, C. X., Su, Z. X., Luo, J., Jiang, L., Shen, S. D., Zheng, W. Y., ... & Chen, Y. J. (2020). Polysaccharide extracted from the leaves of Cyclocarya paliurus (Batal.) Iljinskaja enhanced stress resistance in Caenorhabditis elegans via skn-1 and hsf-1. *International Journal of Biological Macromolecules, 143*, 243–254. https://doi.org/10.1016/j.ijbiomac.2019.12.023

Liu, F., Kan, Q., Feng, K., Chen, Y., Wen, L., He, B., ... & Liu, G. (2023). Process of Zanthoxylum armatum DC. oil by a novel low-temperature continuous phase transition extraction: Evaluation of aroma, pungent compounds and quality. *LWT - Food Science and Technology, 176*, 114523. https://doi.org/10.1016/j.lwt.2023.114523

Liu, Q., Zhang, D. J., & Huang, Q. (2021). Engineering miscellaneous particles from media-milled defatted walnut flour as novel food-grade pickering stabilizers. *Food Research International, 147*, 110554. https://doi.org/10.1016/j.foodres.2021.110554

Mahmood, K., Kamilah, H., Karim, A. A., & Ariffin, F. (2023). Enhancing the functional properties of fish gelatin mats by dual encapsulation of essential oils in β-cyclodextrins/fish gelatin matrix via coaxial electrospinning. *Food Hydrocolloids, 137*, 108324. https://doi.org/10.1016/j.foodhyd.2022.108324

Moniruzzaman, M., Jinnah, M. M., Islam, S., Biswas, J., Al, I., Pramanik, M. J., ... & Zaman, S. (2022). Biological activity of Cucurbita maxima and Momordica charantia seed extracts against the biofilm-associated protein of Staphylococcus aureus: An in vitro and in silico studies. *Informatics in Medicine Unlocked, 33*, 101089. https://doi.org/10.1016/j.imu.2022.101089

Naik, M., Natarajan, V., Modupalli, N., Thangaraj, S., & Rawson, A. (2022). Pulsed ultrasound assisted extraction of protein from defatted bitter melon seeds (*Momardica charantia* L.) meal: Kinetics and quality measurements. *LWT - Food Science and Technology, 155*, 112997. https://doi.org/10.1016/j.lwt.2021.112997

Naik, M., Natarajan, V., Rawson, A., Rangarajan, J., & Manickam, L. (2021). Extraction kinetics and quality evaluation of oil extracted from bitter gourd (*Momardica charantia* L.) seeds using emergent technologies. *LWT - Food Science and Technology*. https://doi.org/10.1016/j.lwt.2020.110714

Nazari, M., Majdi, H., Milani, M., Abbaspour-Ravasjani, S., Hamishehkar, H., & Lim, L.-T. (2019). Cinnamon nanophytosomes embedded electrospun nanofiber: Its effects on microbial quality and shelf-life of shrimp as a novel packaging. *Food Packaging and Shelf Life, 21*, 100349. https://doi.org/10.1016/j.fpsl.2019.100349

Peter, E. L., Kasali, F. M., Deyno, S., Mtewa, A., Nagendrappa, P. B., Tolo, C. U., ... & Sesaazi, D. (2019). *Momordica charantia* L. lowers elevated glycaemia in type 2 diabetes mellitus patients: Systematic review and meta-analysis. *Journal of Ethnopharmacology, 231*, 311–324. https://doi.org/10.1016/j.jep.2018.10.033

Polito, L., Bortolotti, M., Maiello, S., Battelli, M. G., & Bolognesi, A. (2016). Plants producing ribosome-inactivating proteins in traditional medicine. *Molecules*. https://doi.org/10.3390/molecules21111560

Prashantha, M. A. B., Premachandra, J. K., & Amarasinghe, A. D. U. S. (2009). Composition, physical properties and drying characteristics of seed oil of Momordica charantia cultivated in Sri Lanka. *Journal of the American Oil Chemists' Society, 86*(1), 27–32. https://doi.org/10.1007/s11746-008-1319-6

Saadat, S., Emam-Djomeh, Z., & Askari, G. (2021). Antibacterial and Antioxidant gelatin nanofiber scaffold containing ethanol extract of pomegranate peel: Design, characterization and in vitro assay. *Food and Bioprocess Technology, 14*(5), 935–944. https://doi.org/10.1007/s11947-021-02616-z

Shao, P., Liu, Y., Ritzoulis, C., & Niu, B. (2019). Preparation of zein nanofibers with cinnamaldehyde encapsulated in surfactants at critical micelle concentration for active food packaging. *Food Packaging and Shelf Life, 22*, 100385. https://doi.org/10.1016/j.fpsl.2019.100385

Tavassoli-Kafrani, E., Goli, S. A. H., & Fathi, M. (2018). Encapsulation of orange essential oil using cross-linked electrospun gelatin nanofibers. *Food and Bioprocess Technology, 11*(2), 427–434. https://doi.org/10.1007/s11947-017-2026-9

Topuz, F., & Uyar, T. (2020). Antioxidant, antibacterial and antifungal electrospun nanofibers for food packaging applications. *Food Research International, 130*, 108927. https://doi.org/10.1016/j.foodres.2019.108927

Torkamani, A. E., Syahariza, Z. A., Norziah, M. H., Mahmood, W. A. K., & Juliano, P. (2018). Production and characterization of gelatin spherical particles formed via electrospraying and encapsulated with polyphenolic antioxidants from Momordica charantia. *Food and Bioprocess Technology, 11*(11), 1943–1954. https://doi.org/10.1007/s11947-018-2153-y

Torkamani, A. E., Syahariza, Z. A., Norziah, M. H., Wan, A. K. M., & Juliano, P. (2018). Encapsulation of polyphenolic antioxidants obtained from Momordica charantia fruit within zein/gelatin shell core fibers via coaxial electrospinning. *Food Bioscience, 21*, 60–71. https://doi.org/10.1016/j.fbio.2017.12.001

Vairo, C., Vidal, M. V., Hernandez, R. M., Igartua, M., & Villullas, S. (2023). Colistin- and amikacin-loaded lipid-based drug delivery systems for resistant gram-negative lung and wound bacterial infections. *International Journal of Pharmaceutics, 635*, 122739. https://doi.org/10.1016/j.ijpharm.2023.122739

Vutharadhi, S., & Nadimpalli, S. K. (2023). Isolation of Momordica charantia seed lectin and glycosidases from the protein bodies: Lectin-glycosidase (β-hexosaminidase) protein body membrane interaction reveals possible physiological function of the lectin. *Plant Physiology and Biochemistry, 197*, 107663. https://doi.org/10.1016/j.plaphy.2023.107663

Wen, P., Zhu, D.-H., Wu, H., Zong, M.-H., Jing, Y.-R., & Han, S.-Y. (2016). Encapsulation of cinnamon essential oil in electrospun nanofibrous film for active food packaging. *Food Control, 59*, 366–376. https://doi.org/10.1016/j.foodcont.2015.06.005

Wen, P., Zong, M.-H., Linhardt, R. J., Feng, K., & Wu, H. (2017). Electrospinning: A novel nano-encapsulation approach for bioactive compounds. *Trends in Food Science & Technology, 70*, 56–68. https://doi.org/10.1016/j.tifs.2017.10.009

Wu, Z., Wei, J., Jiao, T., Chen, Q., Oyama, M., Chen, Q., & Chen, X. (2022). A lead-based room-temperature phosphorescent metal–organic framework sensor for assessing the peroxide value of edible oils. *Food Chemistry, 385*, 132710. https://doi.org/10.1016/j.foodchem.2022.132710

Yan, J.-K., Wu, L.-X., Qiao, Z.-R., Cai, W.-D., & Ma, H. (2019). Effect of different drying methods on the product quality and bioactive polysaccharides of bitter gourd (*Momordica charantia* L.) slices. *Food Chemistry, 271*, 588–596. https://doi.org/10.1016/j.foodchem.2018.08.012

Yang, H., Wen, P., Feng, K., Zong, M. H., Lou, W. Y., & Wu, H. (2017). Encapsulation of fish oil in a coaxial electrospun nanofibrous mat and its properties. *RSC Advances, 7*(24), 14939–14946. https://doi.org/10.1039/c7ra00051k

Yang, S. B., Rabbani, M. M., Ji, B. C., Han, D. W., Lee, J. S., Kim, J. W., & Yeum, J. H. (2016). Optimum conditions for the fabrication of zein/Ag composite nanoparticles from ethanol/H2O co-solvents using electrospinning. *Nanomaterials*. https://doi.org/10.3390/nano6120230

Yavari Maroufi, L., PourvatanDoust, S., Naeijian, F., & Ghorbani, M. (2022). Fabrication of electrospun polycaprolactone/casein nanofibers containing green tea essential oils: Applicable for active food packaging. *Food and Bioprocess Technology, 15*(11), 2601–2615. https://doi.org/10.1007/s11947-022-02905-1

Yoshime, L. T., de Melo, I. L. P., Sattler, J. A. G., de Carvalho, E. B. T., & Mancini-Filho, J. (2016). Bitter gourd (*Momordica charantia* L.) seed oil as a naturally rich source of bioactive compounds for nutraceutical purposes. *Nutrire, 41*(1), 12. https://doi.org/10.1186/s41110-016-0013-y

Yuan, X., Zhu, X., Zhang, L., Luo, Z., & Zhu, X. (2020). Fundamental insights into walnut shell bio-oil electrochemical conversion: Reaction mechanism and product properties. *BioEnergy Research, 14*(1), 322–332. https://doi.org/10.1007/s12155-020-10155-2

Yun, D., Wang, Z., Li, C., Chen, D., & Liu, J. (2023). Antioxidant and antimicrobial packaging films developed based on the peel powder of different citrus fruits: A comparative study Food. *BioScience*. https://doi.org/10.1016/j.fbio.2022.102319

Zhang, C., Feng, F. Q., & Zhang, H. (2018). Emulsion electrospinning: Fundamentals, food applications and prospects. *Trends in Food Science & Technology, 80*, 175–186. https://doi.org/10.1016/j.tifs.2018.08.005

Zhang, C., Wang, X., Xiao, M., Ma, J. Q., Qu, Y., Zou, L., & Zhang, J. M. (2022). Nano-in-micro alginate/chitosan hydrogel via electrospray technology for orally curcumin delivery to effectively alleviate ulcerative colitis. *Materials & Design*. https://doi.org/10.1016/j.matdes.2022.110894

Zhang, H., Zhang, C., Wang, X., Huang, Y., Xiao, M., Hu, Y. C., & Zhang, J. M. (2022). Antifungal electrospinning nanofiber film incorporated with Zanthoxylum bungeanum essential oil for strawberry and sweet cherry preservation. *LWT - Food Science and Technology*. https://doi.org/10.1016/j.lwt.2022.113992

Zhang, W., Huang, C., Kusmartseva, O., Thomas, N. L., & Mele, E. (2017). Electrospinning of polylactic acid fibres containing tea

tree and manuka oil. *Reactive and Functional Polymers, 117*, 106–111. https://doi.org/10.1016/j.reactfunctpolym.2017.06.013

Zhang, W. M., Liu, R., Sun, X. L., An, H., Min, T. T., Zhu, Z., & Wen, Y. Q. (2022). Leaf-stomata-inspired packaging nanofibers with humidity-triggered thymol release based on thymol/EVOH coaxial electrospinning. *Food Research International, 162*(Pt B), 112093. https://doi.org/10.1016/j.foodres.2022.112093

Zhao, L. C., Zhang, Y., He, L. P., Dai, W. J., Lai, Y. Y., Yao, X. Y., & Cao, Y. (2014). Soy sauce residue oil extracted by a novel continuous phase transition extraction under low temperature and its refining process. *Journal of Agricultural and Food Chemistry, 62*(14), 3230–3235. https://doi.org/10.1021/jf405459v

Zubair, M. F., Atolani, O., Ibrahim, S. O., Oguntoye, O. S., Abdulrahim, H. A., Oyegoke, R. A., & Olatunji, G. A. (2018). Chemical and biological evaluations of potent antiseptic cosmetic products obtained from Momordica charantia seed oil. *Sustainable Chemistry and Pharmacy, 9*, 35–41. https://doi.org/10.1016/j.scp.2018.05.005